*Star Clusters: From the Milky Way to the Early Universe*
*Proceedings IAU Symposium No. 351, 2019*
*A. Bragaglia, M. Davies, A. Sills & E. Vesperini, eds.*

doi:10.1017/S174392131900797X

# Helium variations in Galactic and extragalactic Globular Clusters

**Edoardo P. Lagioia[1], Antonino P. Milone[1], Anna F. Marino[1,2], Aaron Dotter[3], Giacomo Cordoni[1] and Marco Tailo[1]**

[1]Department of Physics and Astronomy, University of Padua,
Via Marzolo 8, 35121, Padua, Italy
email: edoardo.lagioia@unipd.it

[2]Centro di Ateneo di Studi e Attività Spaziali "Giuseppe Colombo" CISAS,
Via Venezia 15, 35131, Padua, Italy

[3]Center For Astrophysics, Harvard & Smithsonian,
60 Garden Street, 02138, Cambridge, MA, USA

**Abstract.** The recent measurements of internal variations of helium in Galactic and extragalactic Globular Clusters (GCs) set binding constraints to the models of formation of Multiple Populations (MPs) in GCs, and gave rise, at the same time, to crucial questions related with the influence of the environment on MP formation as well as with the role played by GCs in the early galactic formation. We present the most recent estimates of helium enrichment in the main populations of a large sample of Galactic and extragalactic GCs.

**Keywords.** globular clusters: general, Hertzsprung-Russel diagram, luminosity function, galaxies: Magellanic Clouds, stars: abundances

## 1. Introduction

Multiple stellar populations (MPs) in old Galactic Globular Clusters (GCs) are characterized by a different content of light elements, with well defined abundance patterns like C-N and Na-O anti-correlations, by different helium mass content ($\delta$Y) and, in few cases, also by different metallicity (for reviews see Gratton *et al.* 2012; Bastian & Lardo 2018; Marino *et al.* 2019).

The determination of internal helium variations in GCs is of primary importance because it provides compelling information on the processes that led to the formation of MPs and, ultimately, gives important clues on the role of the first stars in the reionization of the Universe (see Lagioia *et al.* 2018; Milone *et al.* 2018).

Recently, the discovery of MPs in extragalactic GCs opened up new paths of investigation for the chemical anomalies in clusters with different ages and physical properties.

We exploited multi-wavelength high-resolution *Hubble Space Telescope* (*HST*) observations to perform, for the first time, an homogeneous measurement of $\delta$Y between MPs in a large sample of Galactic GCs, using the luminosity of Red Giant Branch (RGB) bump stars. Moreover, for the first time, we measured light-elements and helium variations in MPs of four extragalactic GCs belonging to the Small Magellanic Cloud (SMC).

We found that Galactic and extragalactic GCs share similar properties, with second generation (2G) stars enhanced in helium and nitrogen, and depleted in carbon and oxygen, with respect to the pristine stellar generation (1G).

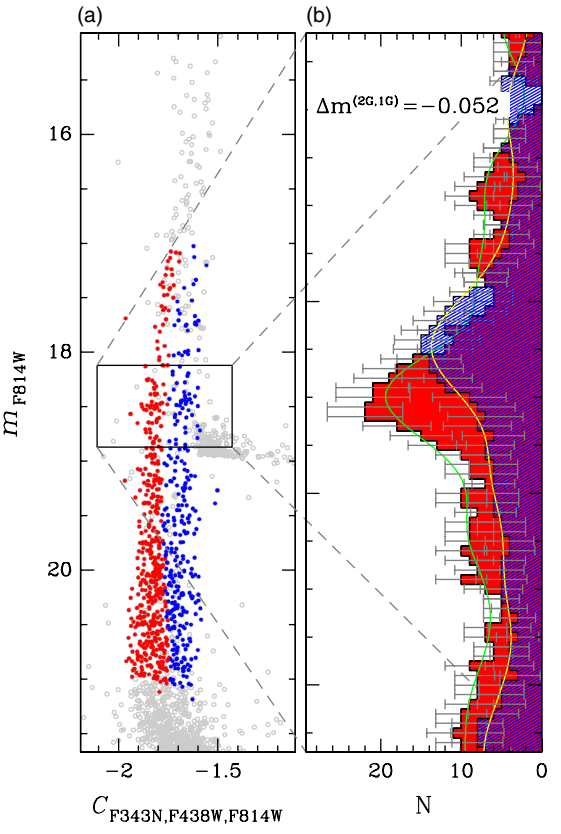


**Figure 1.** *Panel (a)*: $m_{F814W}$ vs. $C_{F343N,F438W,F814W}$ pseudo CMD of the 1G (red; leftmost) and 2G (blue; rightmost) RGB stars of the SMC cluster NGC 121. The black box outlines the RGB bump region. *Panel (b)*: LF of the 1G (leftmost, red histogram) and 2G (rightmost, blue histogram) stars. The peak of the corresponding kernel distributions marks the location of the 1G and 2G RGB bump. Their magnitude displacement, $\Delta m^{(2G,1G)}$, has also been reported on the top.

## 2. The RGB bump of multiple stellar populations

The Ultraviolet (UV) Legacy Survey of Galactic GCs observed 57 clusters in the three broad-band filters F275W, F336W, and F438W, available at the UV and Visual Channel of the Wide Field Camera 3 (WFC3/UVIS) onboard *HST* (Piotto *et al.* 2015). Appropriate combinations of these three bands are at the base of the construction of photometric diagrams suitable for the identification of stellar populations characterized by a different content of light elements (Milone *et al.* 2015). The location of the RGB stars in such diagrams indicates that every cluster has two main stellar populations: the first or 1G, with halo-like content of carbon, nitrogen, and oxygen; the second or 2G, depleted in C and O and enhanced in N with respect to the 1G.

Similar diagrams, but based on the combination of the UVIS/WFC3 narrow-band filter F343N and broad-band filters F336W and F438W, as well as of the ACS/WFC broad-band filters F555W and F814W, allowed us to identify the two main populations in the four Small Magellanic Cloud (SMC) GCs NGC 121, NGC 339, NGC 416 and Lindsay 1 (Lagioia *et al.* 2019).

Thanks to the selection of 1G and 2G stars and by taking advantage of the luminosity function (LF) of the RGB stars, we were able to measure the difference in luminosity between the RGB bump of the single stellar populations for all the Galactic clusters and for the SMC cluster NGC 121. As an example, we show in Figure 1 the procedure to

https://doi.org/10.1017/S174392131900797X Published online by Cambridge University Press

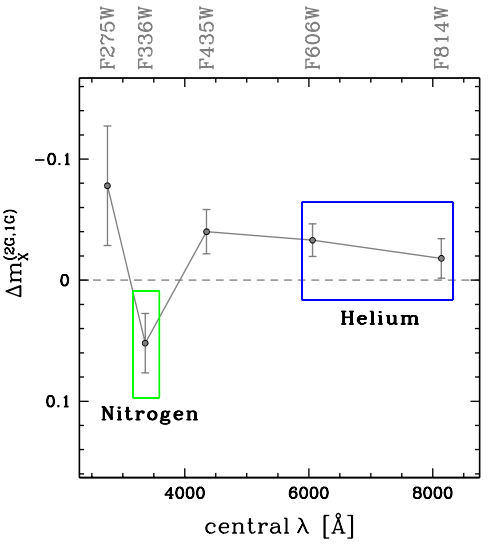


**Figure 2.** Magnitude difference between the RGB bump of 2G and 1G stars of the Galactic GC 47 Tuc in five UVIS/WFC3 filters. The green (leftmost) and blue (rightmost) box highlights the band(s) mostly sensitive to variation of nitrogen and helium, respectively.

select the RGB Bump of 1G and 2G stars of NGC 121. Panel (a) displays the $m_{F814W}$ vs. $C_{F343N,F438W,F814W} = (F343N - F438W) - (F438W - F814W)$ pseudo color-magnitude diagram (CMD) of the RGB of the cluster, where the 1G and 2G stars are represented as red (leftmost) and blue (rightmost) points, respectively. The LF of the 1G and 2G stars in the RGB bump region, outlined by the black box, has been plotted in panel (b). The peaks of the kernel functions, fitting the distributions of the 1G and 2G stars (leftmost, red and rightmost, blue histogram), mark the location of the 1G and 2G RGB bumps. The corresponding magnitude displacement, $\Delta m^{(2G,1G)} = -0.052$ mag, has been also reported. We repeated the same procedure to determine $\Delta m^{(2G,1G)}$ in all the other available bands for this cluster.

By applying a similar procedure to all the Galactic GCs we obtained significant measurements of the RGB bump magnitude difference for 26 out of 57 GCs. As an example, in Figure 2 we plot $\Delta m^{(2G,1G)}$ as a function of the central wavelength of the filter X, with X = F275W, F336W, F438W, F606W and F814W, for the GC NGC 104 (47 Tuc). The dip visible in correspondence of the band F336W is largely due to nitrogen enhancement of 2G stars with respect to the 1G stars, as highlighted by the green (leftmost) box. On the other hand, as a consequence of the change of the effective temperature of a star, hence of its luminosity at a given evolutionary stage, the effects of helium variations are mostly visible in optical bands, as highlighted by the blue (rightmost) box.

By means of synthetic spectral analysis, we estimated the contribution due to light-elements variation to the observed scatter in optical bands. Finally, by using appropriate theoretical models, we obtained an estimate of $\delta Y$ corresponding to the observed RGB bump magnitude displacements, for all the GCs with [Fe/H] $< -1.0$ dex. As shown by the dashed gray histogram in Figure 3, we found that the mean value of the distribution of the helium variation between 2G and 1G stars, for the final selection of 18 Galactic GCs, is $\delta Y \approx 0.01$. In the case of the SMC cluster NGC 121 we found $\delta Y = 0.026 \pm 0.009$.

## 3. Color spread of multiple populations in SMC clusters

Since the RGB bump is not detectable for NGC 339, NGC 416 and Lindsay 1, we adopted a different method to measure the internal helium variation for these SMC clusters and extended the procedure also to NGC 121.

https://doi.org/10.1017/S174392131900797X Published online by Cambridge University Press

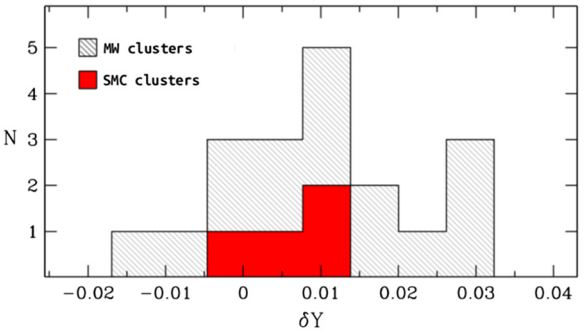


**Figure 3.** Distribution of the helium abundance variation between the two main populations of 18 Galactic GCs (Lagioia *et al.* 2018; dashed gray histogram) and of four SMC clusters (Lagioia *et al.* 2019; solid red histogram).

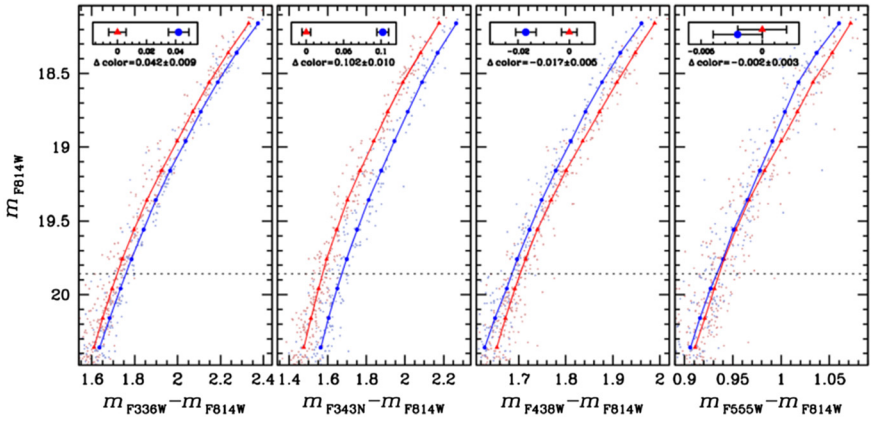


**Figure 4.** CMDs in different color combinations, for the RGB stars of the cluster NGC 121. Fiducial lines have been overplotted. The dashed line marks the reference magnitude, $m_{\rm ref}$, along the fiducial lines. The inset in each panel displays the difference in the relative color between the points at $m_{\rm ref}$, along the two fiducials.

As shown in the four CMDs relative to the cluster NGC 121, in Fig. 4, we built the ridge line of the RGB sequence of each population, in all the possible color combinations, and measured the difference between the color of the points along the fiducials, at a reference magnitude, $m_{\rm ref} = m^{MSTO}_{F814W} - 2$, where $m^{MSTO}_{F814W}$ is the main sequence turn-off magnitude in F814W band.

As done in the case of the RGB bump, we determined, by means of synthetic spectra analysis, the contribution of light-elements variation to the observed color spread. Finally, appropriate theoretical models allowed us to estimate the difference in helium mass content between the two main stellar populations corresponding to the color difference observed in optical bands.

The solid red histogram in Fig. 3 shows that the four SMC clusters have helium variations similar to those observed for the Galactic GCs, with 2G stars enhanced in helium by $\delta$Y $\sim 0.01$. In particular, for NGC 121 we found $\delta$Y $\sim 0.009 \pm 0.006$, a value consistent within $1.5\,\sigma$ with that found by using the RGB bump displacement. We also found that 2G stars in the four SMC clusters are depleted in carbon and/or oxygen (Lagioia *et al.* 2019)

https://doi.org/10.1017/S174392131900797X Published online by Cambridge University Press

These findings provide evidence that old Galactic and intermediate and old extragalactic GCs show consistent internal helium variations and seem to share the same chemical properties, with helium-rich stars being N-rich and possibly C-O poor, thus suggesting an universal mechanism at the base of the formation of multiple populations at high redshifts.

## References

Bastian, N. & Lardo, C. 2018, *ARA&A*, 56, 83B
Gratton, R. G., Carretta, E., & Bragaglia, A. 2012, *A&ARv*, 20, 50
Lagioia, E. P., Milone, A. P., Marino, A. F., *et al.* 2018, *MNRAS*, 475, 4088
Lagioia, E. P., Milone, A. P., Marino, A. F., *et al.* 2019, *ApJ*, 871, 140
Marino, A. F., Milone, A. P., Renzini, A., *et al.* 2019, *MNRAS*, 487, 3815
Milone, A. P., Marino, A. F., Piotto, G., *et al.* 2015, *ApJ*, 808, 51
Milone, A. P., Marino, A. F., Renzini, A., *et al.* 2018, *MNRAS*, 481, 5098
Piotto, G., Milone, A. P., Bedin, L. R., *et al.* 2015, *AJ*, 149, 91

https://doi.org/10.1017/S174392131900797X Published online by Cambridge University Press